Photoisomerization of a rotaxane hydrogen bonding template: Light-induced acceleration of a large amplitude rotational motion

Francesco G. Gatti*, Salvador León†, Jenny K. Y. Wong*, Giovanni Bottari*, Andrea Altieri*, M. Angeles Farran Morales*, Simon J. Teat‡, Céline Frochot§, David A. Leigh*¶, Albert M. Brouwer§¶, and Francesco Zerbetto†¶

*School of Chemistry, University of Edinburgh, The King's Buildings, West Mains Road, Edinburgh EH9 3JJ, United Kingdom; †Dipartimento di Chimica ''G. Ciamician,'' Università degli Studi di Bologna, V. F. Selmi 2, 40126, Bologna, Italy; ‡Central Laboratory of the Research Councils Daresbury Laboratory, Warrington WA4 4AD, United Kingdom; and §Laboratory of Organic Chemistry, University of Amsterdam, Nieuwe Achtergracht 129, NL-1018 WS Amsterdam, The Netherlands

Establishing methods for controlling aspects of large amplitude submolecular movements is a prerequisite for the development of artificial devices that function through rotary motion at the molecular level. Here we demonstrate that the rate of rotation of the interlocked components of fumaramide-derived [2]rotaxanes can be accelerated, by >6 orders of magnitude, by isomerizing them to the corresponding maleamide [2]rotaxanes by using light.

molecular machines | dynamics

Large amplitude internal rotations that resemble to some extent processes found in authentic machinery have recently inspired analogic molecular versions of gears (1), turnstiles (2), brakes (3), ratchets (4, 5), rotors (6), and unidirectional spinning motors (7–10) and are an inherent characteristic of many catenanes and rotaxanes (11–13). Establishing methods for controlling aspects of such movements is a prerequisite for the development of artificial devices that function through rotary motion at the molecular level.‖ In this regard, we recently reported the unexpected discovery that the rate of rotation of the interlocked components of benzylic amide macrocycle-containing nitrone and fumaramide [2]rotaxanes can be slowed (''dampened'') by 2–3 orders of magnitude by applying a modest ($\approx$1 V·cm^{-1}) external oscillating electric field (14). Here we demonstrate that the rate of rotation of the interlocked components of the olefin-based rotaxanes can also be accelerated, by >6 orders of magnitude, using another broadly useful stimulus, light.

Fumaramide threads template the assembly of benzylic amide macrocycles around them to form rotaxanes in high yields (15). This cheap and simple preparative procedure (suitable threads are prepared in a single step from fumaryl chloride and a bulky primary or secondary amine) is particularly efficient because the trans-olefin fixes the two hydrogen bond-accepting groups of the thread in an arrangement that is complementary to the geometry of the hydrogen bond-donating sites of the forming macrocycle. However, the feature of the fumaramide unit that makes it such an effective template also provides an opportunity to enforce a geometrical change in the thread <u>after</u> rotaxane formation, thus altering the nature and strength of the interactions between the interlocked components. Isomerization of the olefin from *E*- to *Z*- must necessarily disrupt the near-ideal hydrogen bonding motif between macrocycle and thread and therefore also change any internal dynamics governed by those interactions.

To test this idea, the photochemical isomerization of three fumaramide-based threads (*E*-1–3) and rotaxanes (*E*-4–6) was investigated. The synthesis of rotaxanes *E*-4 and *E*-6 has been described (15), and *E*-5 was prepared in analogous fashion from the corresponding thread, *E*-2, isophthaloyl dichloride and *p*-xylylene diamine (Scheme 1).** Under the same reaction conditions the cis-olefin (maleamide) threads, *Z*-1–3, did not give detectable quantities of the corresponding *Z*-rotaxanes.

Experimental Procedures

General Method for the Photoisomerization of Fumaramide [2]Rotaxanes. The rotaxanes *E*-4–6 (0.60 g) were dissolved in CH$_2$Cl$_2$ [except for solubility reasons *E*-6, MeOH/CHCl$_3$ (1/9)] in a quartz vessel. The solutions were directly irradiated at 254 nm by using a multilamp photoreactor model MLU18 manufactured by Photochemical Reactors (Reading, U.K.). The progress of photoisomerization was monitored by TLC (silica, CHCl$_3$/EtOAc 4:1) or ^{1}H NMR. The different photostationary states were reached in a range of times not exceeding 30 min after which the reaction mixture was concentrated under reduced pressure to afford the crude products (*Z*-4–6). The unconverted trans isomers were isolated by triturating the solids with PhMe/CH$_2$Cl$_2$ (1:1, $\approx$20 ml) and, because the photoisomerization process produces few byproducts, could be recycled, eventually leading to >90% conversion of each rotaxane to the corresponding cis-isomer. The solutions were then passed through a pad of silica (CHCl$_3$/EtOAc, 4:1) to afford the cis isomers *Z*-4–6 in 50%, 47%, and 45% yields, respectively, from a single photoisomerization experiment.

Other Procedures. Experimental procedures for the synthesis of *Z*-5, x-ray crystallography of *E*-5 and *Z*-5, and selected charac-
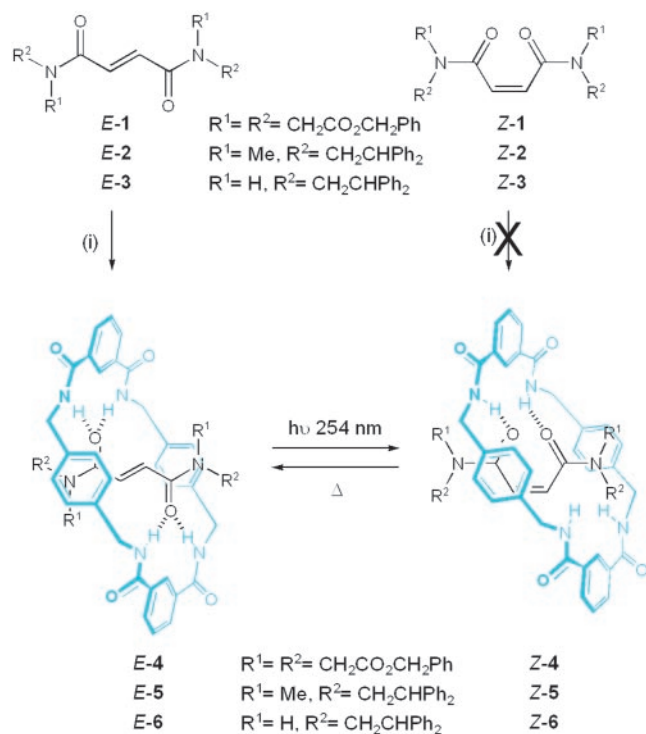

‖Speculation over the possible utility of submolecular rotation in synthetic molecular structures ranges from ''gearing'' systems, where controlled motion in one part of a molecule brings about changes in conformation in another (e.g., to generate catalysts with rotating binding sites, in analogy to F$_1$-ATPase, etc.), to systems that rotate functional groups on surfaces, or in the bulk, to bring about changes in local or macroscopic characteristics (11, 23). Indeed, for wonderful examples of the use of submolecular rotational motion to bring about property changes in materials, see refs. 24 and 25. Examples of specifically controlling the frequency of large amplitude internal rotary motions include the redox-mediated acceleration/deceleration of the spinning of porphyrin ligands in cerium and zirconium sandwich complexes (26), the environment-dependant rate of circumrotation in hydrogen bonded [2]catenanes (27), and the electrochemically induced pirouetting of a macrocycle in a rotaxane (28).

**The modest yield (33%) of *E*-5 is probably a consequence of the {*E*,*E*}- and/or {*E*,*Z*}-tertiary amide rotamers being sterically mismatched with the forming macrocycle. Interestingly, a small amount (2%) of rotaxane *E*-6, presumably arising from *p*-xylylene diamine-catalyzed isomerization of the thread, was isolated from the reaction of pristine *Z*-3, again exemplifying the extraordinary efficiency of the *E*-3 template for rotaxane formation.

Scheme 1. Synthesis of [2]rotaxanes *E/Z*-**4**–**6**. (*i*) Four equivalents isophthaloyl dichloride, four equivalents *p*-xylylene diamine, Et$_3$N, 4 h, high dilution; CHCl$_3$ for *E*-**4** (67%) and *E*-**5** (33%), 1/9 MeCN/CHCl$_3$ for *E*-**6** (97%). Direct irradiation (254 nm, 30 min) of a solution of an *E*-rotaxane (0.1 M, room temperature, CH$_2$Cl$_2$ [1:9 MeOH/CHCl$_3$ for *E*-**6**]) yields the ''accelerated'' *Z*-isomer (45–50% single experiment; >90% from four successive cycles). Heating a 0.02 M solution of a *Z*-rotaxane at 400 K reforms the ''dampened'' *E*-isomer (*E*-**6**: C$_2$D$_2$Cl$_4$, 7 days, 84% or *d$_6$*-DMSO, 4 days, 100%).
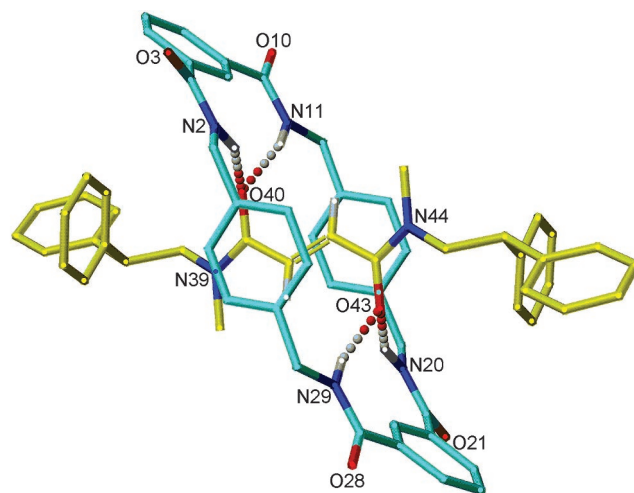
Fig. 1. X-ray crystal structure of [2]rotaxane *E*-**5** (for clarity, carbon atoms of the macrocycle are shown in blue and the carbon atoms of the thread in yellow; oxygen atoms are depicted in red, nitrogen atoms are dark blue, and selected hydrogen atoms are white). Intramolecular hydrogen bond distances (Å): O40−HN2/O43−HN20 = 2.22, O40−HN11/O43−HN29 = 1.94.

terization data for *Z*-**5** and *E*-**4**–**6** are provided as *Supporting Text*, which is published as supporting information on the PNAS web site, www.pnas.org.

Results and Discussion

Single crystals suitable for investigation by x-ray crystallography were obtained for each of the three *E*-rotaxanes. In each case the solid-state structure shows two sets of bifurcated hydrogen bonds between the amide groups of the macrocycle and the carbonyl groups of the fumaramide system (15). The crystal structure of *E*-**5** is typical (Fig. 1) and shows the macrocycle in a chair conformation forming short, close-to-linear, hydrogen bonds orthogonal to the lone pairs of the fumaramide carbonyl groups. Of the three different tertiary amide rotamers present in solution (as observed by NMR) only the {ZZ}amide rotamer of *E*-**5** is found in the crystal.

All three fumaramide threads *E*-**1**–**3** and rotaxanes *E*-**4**–**6** smoothly undergo photoisomerization (16, 17) (254 nm; 0.1 M solution in CH$_2$Cl$_2$ or, for solubility reasons in the case of *E*-**6**, 1:9 MeOH/CHCl$_3$; 30 min) to the corresponding maleamide (*Z*-olefin) systems. The yields for the rotaxanes, 45–50%, are remarkably good considering the confined cavity that the molecular rearrangement has to occur in and that the intercomponent hydrogen bonding between the thread and macrocycle is complementary to the positions of the amide groups only in the *E*-olefin. Unanticipated enhanced solubility of the *Z*-rotaxanes in nonpolar solvents allowed the separation of the *E/Z* photochemical reaction mixtures into the individual isomers by simple trituration (PhMe/CH$_2$Cl$_2$, 1:1). The photoisomerization reaction produces few byproducts so *E*-rotaxanes recovered in this

way could be recycled, leading to >90% overall conversion to the *Z*-isomer from a series of irradiation experiments.

The ^{1}H NMR spectra of each pair of *E*- and *Z*-olefin rotaxanes gives insight regarding their structure and relative dynamic properties in nonpolar solvents. The trends are similar in all cases but the clearest information is provided by *E/Z*-**4**.[††]

The variable temperature ^{1}H NMR spectra of *E*-**4** and *Z*-**4** in CD$_2$Cl$_2$ (223–273 K) and C$_2$D$_2$Cl$_4$ (339–393 K) are shown in Fig. 2 (the wide temperature range involved meant different nonhydrogen bond-disrupting solvents were required to monitor the dynamic processes at high and low temperatures). Pirouetting, a 180° rotation of the macrocycle about the axis of the arrow plus formal chair–chair flip of the macrocycle, is the simplest process that must occur to translate the equatorial macrocycle methylene protons, H$_{E2}$, onto the axial, H$_{E1}$, sites. In the fumaramide system the H$_E$ protons coalesce at 273 K and are fully resolved into the H$_{E1}$ and H$_{E2}$ resonances at 223 K (Fig. 2*a*). The coupling constants confirm the axial and equatorial assignments of H$_{E1}$ and H$_{E2}$. Spin polarization transfer by selective inversion recovery experiments provided a direct measure of the rate of the exchange process I (i.e., half circumrotation of the macrocycle) at 298 K corresponding to an energy barrier $\Delta G^{\ddagger} = 13.4 \pm 0.1$ kcal·mol^{-1}, which extrapolates to a rate of macrocycle rotation of ≈ 1 s^{-1} at 223 K (15). In contrast, the macrocycle methylene protons (H$_E$) in *Z*-**4** remain sharp and well resolved throughout this temperature range and only begin to broaden significantly at 223 K (Fig. 2*b*); remarkably, the broadening of H$_E$ in *Z*-**4** at 223 K is comparable to that in *E*-**4** at 359 K, a 136° temperature difference between the two rotaxane isomers! Exchange is so fast in *Z*-**4** that it is not possible to resolve the signals and prove unequivocally by experiment that the process responsible for the broadening at this temperature is, in fact, macrocycle

---

[††]The spectra of *Z*-**6** are complicated because intracomponent hydrogen bonding of the maleamide group desymmetrizes the rotaxane (the macrocycle methylene groups appear as an ABX system because the two faces of the macrocycle experience different environments). Similarly, the temperature-dependent equilibrium between the populations of the different amide rotamers present in the methylated rotaxanes *E/Z*-**5** makes their study nontrivial, whereas the symmetrical tertiary amides means *E/Z*-**4** suffers no such complication. For a discussion of the effect of the different strengths of intercomponent hydrogen bonding in *E*-**4** and *Z*-**4** on the dynamics of amide rotamerization, see *Supporting Text*.
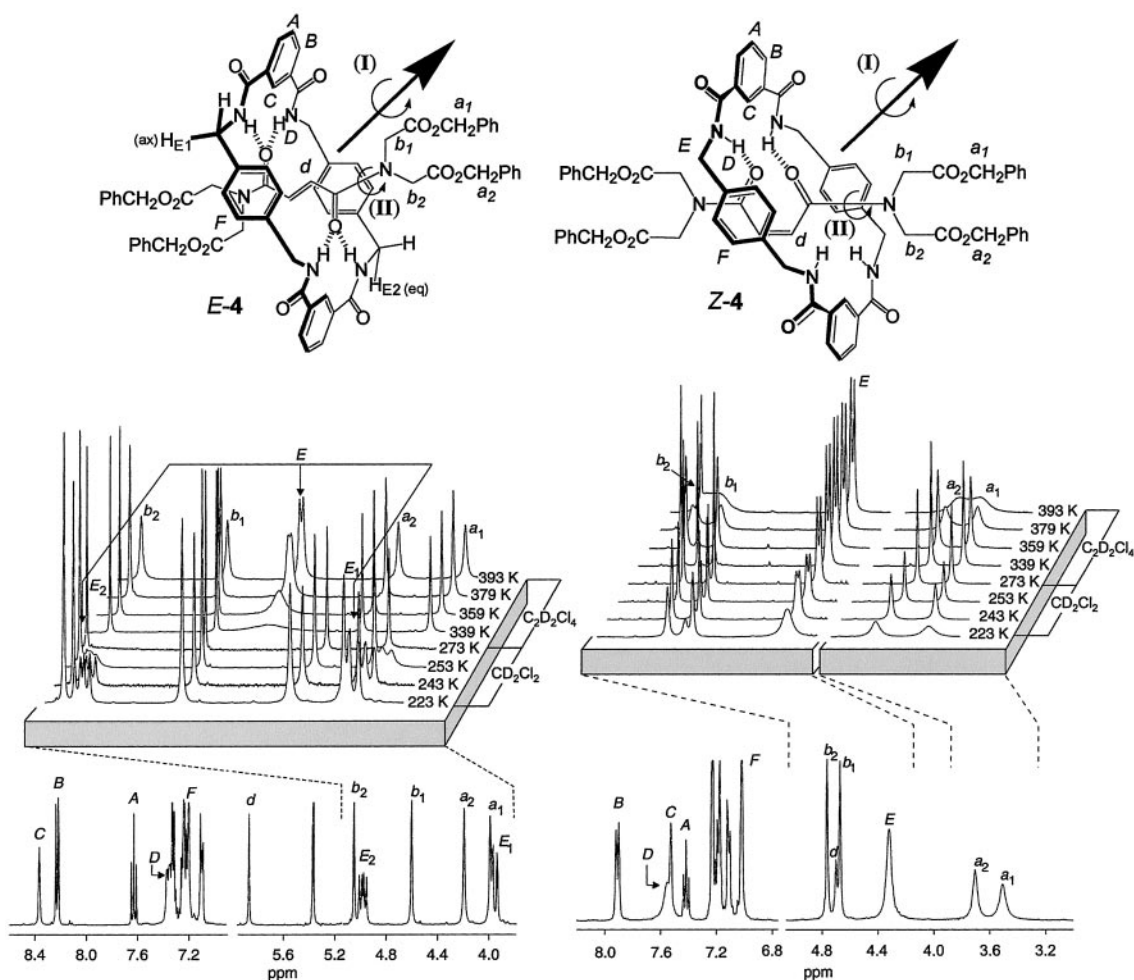
Fig. 2. Variable temperature ^{1}H NMR spectra (400 MHz) of *E*-4 (*a*) and *Z*-4 (*b*) in CD$_2$Cl$_2$ at 223 K (main traces) and 223–273 K (stackplot expansions) and C$_2$D$_2$Cl$_4$ at 339–393 K (stackplot expansions). Lettering corresponds to selected nonequivalent proton environments. A 180° rotation of the macrocycle about the axis of the arrow, plus chair–chair flipping of the macrocycle, translates the H$_{E2}$ (equatorial) protons onto the H$_{E1}$ (axial) sites. The NMR spectra in *a* reveal slow pirouetting of the macrocycle about the thread in *E*-4 (H$_{E1}$ and H$_{E2}$ coalesce at 273 K, $\Delta G^\ddagger = 13.4 \pm 0.1$ kcal·mol^{-1}; process I) and slow rotation of the thread tertiary amide bonds (H$_{a1}$ and H$_{a2}$/H$_{b1}$ and H$_{b2}$ fully resolved even at 393 K, $\Delta G^\ddagger = 21.1 \pm 0.1$ kcal·mol^{-1}; process II). The NMR spectra in *b* show that process I is much lower in energy for *Z*-4 ($\Delta G^\ddagger = 6.8 \pm 0.8$ kcal·mol^{-1}) than *E*-4 and that process II is also more facile (H$_{a1}$ and H$_{a2}$/H$_{b1}$ and H$_{b2}$ broadening at higher temperatures, $\Delta G^\ddagger = 20.0 \pm 0.1$ kcal·mol^{-1}) (30).

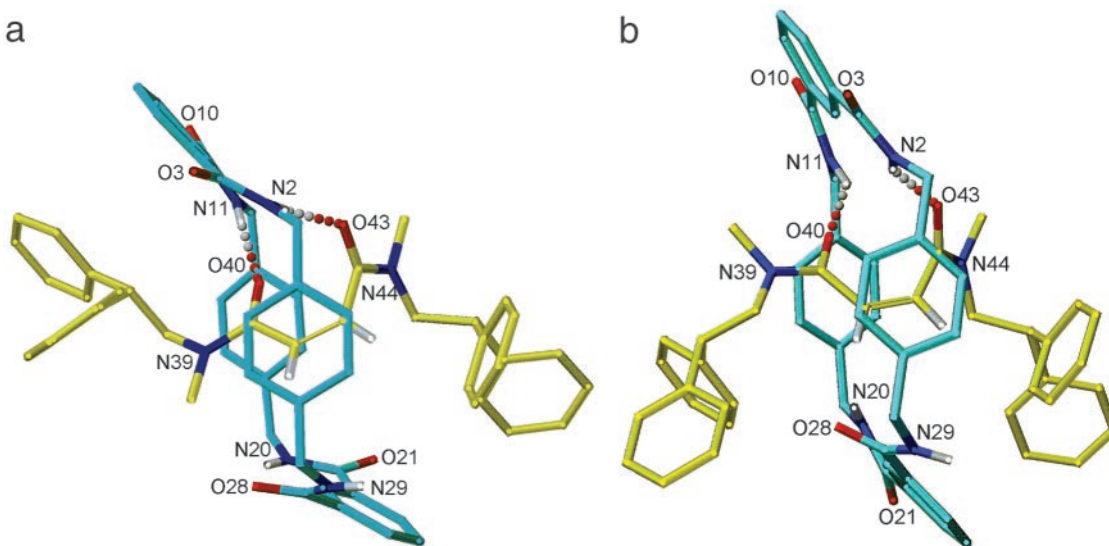**Fig. 3.** X-ray crystal structures of {*ZE*} (*a*) and {*EE*} (*b*) rotamers of *N,N′*-dimethylmaleamide [2]rotaxane *Z*-5. Intramolecular hydrogen bond distances (Å): (*a*) O40-HN11 = 2.08, O43-HN2 = 2.05; (*b*) O40-HN11 = 1.76, O43-HN2 = 2.08.
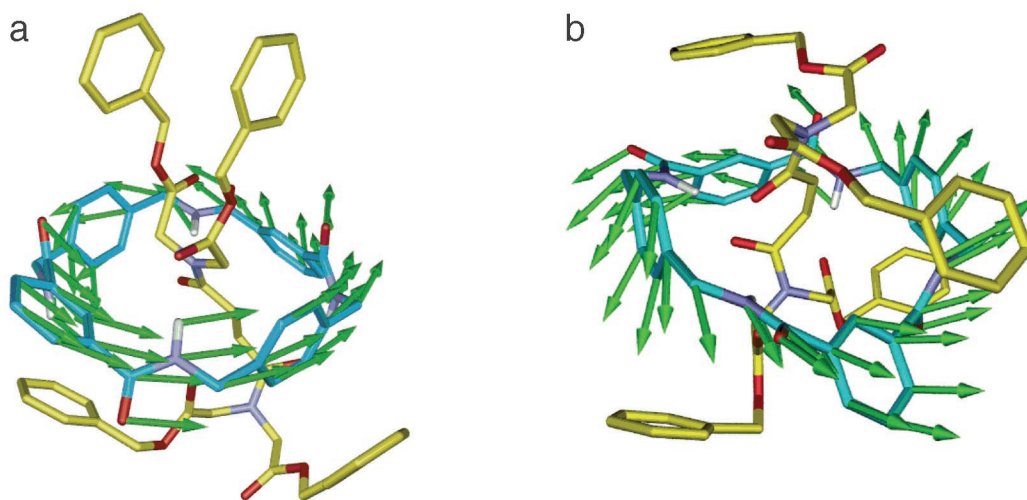
Fig. 4. Calculated transition-state structures for the macrocycle ring motions for rotaxanes *Z*-**4** (*a*) and *E*-**4** (*b*). Green arrows represent the corresponding atomic motion vectors connecting the transition states to their minima.

pirouetting (it could be occurring at even lower temperatures). However, making the assumption (see below) that this is the process responsible for broadening, line shape analysis gives an energy barrier of 6.8 ± 0.8 kcal·mol^{-1}, i.e., a macrocycle spinning rate $>1.2 \times 10^6$ s^{-1} at 223 K.

Remarkably, it was possible to obtain an x-ray crystal structure of one of the rotaxanes with a "switched off" recognition motif. Small crystals of *Z*-**5** suitable for investigation with a synchrotron source were grown from slow evaporation of a saturated solution in CHCl$_3$/MeOH. In contrast to the crystal structure of *E*-**5**, two of the three tertiary amide rotamers, i.e., {*ZE*} and {*EE*} rotamers, are present in the unit cell of *Z*-**5** (Fig. 3 *a* and *b*, respectively). Both forms are consistent with the dramatic increase in the rate of rotation in solution for the cis-rotaxanes observed experimentally by ^{1}H NMR spectroscopy; the consequence of isomerizing the double bond is that the amide groups of the thread are held in positions such that they can hydrogen-bond to only one of the two isophthalamide groups of the macrocycle. It is interesting to note that the energy barrier for the trans-rotaxane with four intercomponent hydrogen bonds (13.4 kcal·mol^{-1}) is almost exactly twice the value for the cis-rotaxane with two inter-component hydrogen bonds (≈ 6.8 kcal·mol^{-1}).

To obtain a more detailed understanding of the dynamic properties of these systems and, in particular, to confirm that the low energy dynamic process measured by NMR in the maleam-

ide rotaxane was circumrotation, we carried out simulations of the dynamic processes present in both *E*-**4** and *Z*-**4**.

Using a computational procedure that uses the MM3 force-field (18) and the TINKER program (19) and has proved successful in describing the circumrotation pathway in catenanes (20), macrocycle pirouetting in rotaxanes (13), and other properties in mechanically interlocked molecules (21, 22), it was possible to locate the saddle points for macrocycle circumrotation in *E*-**4** and *Z*-**4**. Fig. 4 shows the transition states, the arrows indicating the initial motion that the macrocycle would undergo away from the saddle point (arrows showing the movement of the thread are not shown for clarity). The calculated activation energies (13.51 kcal·mol^{-1} for *E*-**4** and 6.53 kcal·mol^{-1} for *Z*-**4**) compare well with the NMR-determined ΔGs of 13.4 ± 0.1 and 6.8 ± 0.8 kcal·mol^{-1}, respectively, and thus confirm that macrocycle pirouetting is probably a major contributor to the broadening of resonances observed in the low-temperature NMR spectra of *Z*-**4**. The good agreement of calculations and experiments also allows one to take a closer look at the contributions of various kinds of interactions to the dynamic process of pirouetting. Table 1 shows the different energy contributions to the *E*-**4** and *Z*-**4** minima and transition states. Interestingly, from the calculations the ≈ 7 kcal·mol^{-1} difference between the activation barriers of circumrotation in the two molecules can be ascribed to contributions from all the energy components, not just H bonding.

Preliminary studies show that it is possible to reverse the photoisomerization process thermally. Heating each of *Z*-**4**–**6** (C$_2$D$_2$Cl$_4$ or *d*$_6$-DMSO, 400 K, 4–7 days) resulted in reconversion to the more thermodynamically stable *E*-rotaxanes in good-to-excellent (80–100%) yields. Other simple cis-trans olefin inter-conversion reactions are currently being investigated.[‡‡]

The post-assembly photoconversion of a precise hydrogen-bonding, rotaxane-forming template to a motif that does not template the formation of mechanical bonds is unprecedented. The resulting mismatch in recognition sites between macrocycle and thread dramatically reduces the energy barrier to macro-cycle pirouetting in the rotaxane. Such control could be useful for the future construction of synthetic molecular machines that use large amplitude internal rotary motions.

Table 1. Calculated contributions to the rotaxane energy minima and transition states

	E_v	$E_{\text{H-bonding}}$	$E_{\pi\text{-stacking}}$	E_{vdW}
E-**4***	29.18	−20.14	−15.36	−24.91
E-**4**[†]	33.09 (3.91)	−13.75 (6.39)	−12.65 (2.71)	−24.40 (0.51)
Z-**4***	38.11	−16.84	−14.89	−30.97
Z-**4**[†]	44.66 (6.55)	−15.99 (0.85)	−16.73 (−1.84)	−29.99 (0.98)

Molecular energy contributions (kcal·mol^{-1}) divided into four components: a valence term, E_v, which includes stretchings and in-plane and out-of-plane bendings; a hydrogen bond contribution, $E_{\text{H-bonding}}$; π-π stacking energy, $E_{\pi\text{-stacking}}$; and the remaining van der Waals components, E_{vdW}. The energy differences between the minima and the transition states are given in parentheses.
*Energy minimum.
[†]Transition state energy.

1. Iwamura, H. & Mislow, K. (1988) *Acc. Chem. Res.* **21,** 175–182.
2. Bedard, T. C. & Moore, J. S. (1995) *J. Am. Chem. Soc.* **117,** 10662–10671.
3. Kelly, T. R., Bowyer, M. C., Bhaskar, K. V., Bebbington, D., Garcia, A., Lang, F., Kim, M. H. & Jette, M. P. (1994) *J. Am. Chem. Soc.* **116,** 3657–3658.
4. Kelly, T. R., Tellitu, I. & Sestelo, J. P. (1997) *Angew. Chem. Int. Ed. Engl.* **36,** 1866–1868.
5. Kelly, T. R., Sestelo, J. P. & Tellitu, I. (1998) *J. Org. Chem.* **63,** 3655–3665.
6. Schoevaars, A. M., Kruizinga, W., Zijlstra, R. W. J., Veldman, N., Spek, A. L. & Feringa, B. L. (1997) *J. Org. Chem.* **62,** 4943–4948.
7. Kelly, T. R., De Silva, H. & Silva, R. A. (1999) *Nature* **401,** 150–152.
8. Koumura, N., Zijlstra, R. W. J., van Delden, R. A., Harada, N. & Feringa, B. L. (1999) *Nature* **401,** 152–155.
9. Kelly, T. R., Silva, R. A., De Silva, H., Jasmin, S. & Zhao, Y. (2000) *J. Am. Chem. Soc.* **122,** 6935–6949.
10. Koumura, N. L., Geertsema, E. M., van Gelder, M. B., Meetsma, A. & Feringa, B. L. (2002) *J. Am. Chem. Soc.* **124,** 5037–5051.
11. Balzani, V., Credi, A., Raymo, F. M. & Stoddart, J. F. (2000) *Angew. Chem. Int. Ed.* **39,** 3348–3391.
12. Stoddart, J. F., ed. (2001) *Acc. Chem. Res.* **34,** 409–522.
13. Sauvage, J.-P., ed. (2001) *Molecular Machines and Motors: Structure and Bonding* (Springer, Berlin), Vol. 99.
14. Bermudez, V., Capron, N., Gase, T., Gatti, F. G., Kajzar, F., Leigh, D. A., Zerbetto, F. & Zhang, S. (2000) *Nature* **406,** 608–611.
15. Gatti, F. G., Leigh, D. A., Nepogodiev, S. A., Slawin, A. M. Z., Teat, S. J. & Wong, J. K. Y. (2001) *J. Am. Chem. Soc.* **123,** 5983–5989.
16. Campari, G., Fagnoni, M., Mella, M. & Albini, A. (2000) *Tetrahedron Asym.* **11,** 1891–1906.
17. Frkanec, L., Jokic, M., Makarevic, J., Wolsperger, K. & Zinic, M. (2002) *J. Am. Chem. Soc.* **124,** 9716–9717.
18. Allinger, N. L., Yuh, Y. H. & Lii, J.-H. (1989) *J. Am. Chem. Soc.* **111,** 8551–8556.
19. Dudek, M. J. & Ponder, J. (1995) *J. Comput. Chem.* **16,** 791–816.
20. Deleuze, M. S., Leigh, D. A. & Zerbetto, F. (1999) *J. Am. Chem. Soc.* **121,** 2364–2379.
21. Biscarini, F., Cavallini, C., Leigh, D. A., León, S., Teat, S. J., Wong, J. K. W. & Zerbetto, F. (2002) *J. Am. Chem. Soc.* **124,** 225–233.
22. Fustin, C.-A., Leigh, D. A., Rudolf, P., Timpel, D. & Zerbetto, F. (2000) *ChemPhysChem* **1,** 97–100.
23. Vacek, J. & Michl, J. (1997) *New J. Chem.* **21,** 1259–1268.
24. van Delden, R. A., Koumura, N., Harada, N. & Feringa, B. L. (2002) *Proc. Natl. Acad. Sci. USA* **99,** 4945–4949.
25. Collier, C. P., Mattersteig, G., Wong, E. W., Luo, Y., Beverly, K., Sampaio, J., Raymo, F. M., Stoddart, J. F. & Heath, J. R. (2000) *Science* **289,** 1172–1175.
26. Tashiro, K., Konishi, K. & Aida, T. (2000) *J. Am. Chem. Soc.* **122,** 7921–7926.
27. Leigh, D. A., Murphy, A., Smart, J. P., Deleuze, M. S. & Zerbetto, F. (1998) *J. Am. Chem. Soc.* **120,** 6458–6467.
28. Raehm, L., Kern, J.-M. & Sauvage, J.-P. (1999) *Chem. Eur. J.* **5,** 3310–3317.
29. Chatterjee, S., Pedireddi, V. R. & Rao, C. N. R. (1998) *Tetrahedron Lett.* **39,** 2843–2846.
30. Clegg, W., Gimenez-Saiz, C., Leigh, D. A., Murphy, A., Slawin, A. M. Z. & Teat, S. J. (1999) *J. Am. Chem. Soc.* **121,** 4124–4129.